Stem Cell Reports
Article

ISSCR

OPEN ACCESS

# In Vivo RNAi Screen Unveils PPARγ as a Regulator of Hematopoietic Stem Cell Homeostasis

Mathieu Sertorio,[1] Wei Du,[1] Surya Amarachintha,[1] Andrew Wilson,[1] and Qishen Pang[1,*]
[1]Division of Experimental Hematology and Cancer Biology, Cincinnati Children's Hospital Medical Center, Cincinnati, OH 45229, USA
*Correspondence: qishen.pang@cchmc.org
http://dx.doi.org/10.1016/j.stemcr.2017.03.008

## SUMMARY

Hematopoietic stem cell (HSC) defects can cause repopulating impairment leading to hematologic diseases. To target HSC deficiency in a disease setting, we exploited the repopulating defect of Fanconi anemia (FA) HSCs to conduct an in vivo short hairpin RNA (shRNA) screen. We exposed *Fancd2*$^{-/-}$ HSCs to a lentiviral shRNA library targeting 947 genes. We found enrichment of shRNAs targeting genes involved in the PPARγ pathway that has not been linked to HSC homeostasis. PPARγ inhibition by shRNA or chemical compounds significantly improves the repopulating ability of *Fancd2*$^{-/-}$ HSCs. Conversely, activation of PPARγ in wild-type HSCs impaired hematopoietic repopulation. In mouse HSCs and patient-derived lymphoblasts, PPARγ activation is manifested in upregulating the p53 target p21. *PPARγ* and co-activators are upregulated in total bone marrow and stem/progenitor cells from FA patients. Collectively, this work illustrates the utility of RNAi technology coupled with HSC transplantation for the discovery of novel genes and pathways involved in stress hematopoiesis.

## INTRODUCTION

Hematopoietic stem cells (HSCs) are a distinct population of multipotent cells that can self-renew and differentiate into various types of blood cells and thus are responsible for maintenance and homeostasis of a healthy hematopoietic system (Morrison et al., 1995; Orford and Scadden, 2008; Orkin and Zon, 2008). HSCs are exposed daily to internal and external stresses which in turn lead to DNA damage. Accumulation of DNA damage in hematopoietic stem and progenitor cells (HSPCs) during the cell's life span is a factor of hematopoietic system aging and degeneration, and likely contributes to transformation and cancer development (Rossi et al., 2008). Accelerated bone marrow (BM) degeneration leading to BM failure and high risks of leukemia development is frequently observed in diseases with a deficiency in DNA repair pathways such as Fanconi anemia (FA) (Taniguchi and D'Andrea, 2006).

FA is an inherited disease caused by mutations in any of 17 already identified FA DNA repair pathway genes (*FANCA-S*) (Kottemann and Smogorzewska, 2013; Sawyer et al., 2015). FA proteins have been mainly studied for their role in genomic DNA repair and genome integrity. Upon DNA damage, eight of the FA proteins (FANCA, -B, -C, -E, -F, -G, -L, and -M) interact to form the FA core complex responsible for FANCD2 and FANCI activation by mono-ubiquitination (Kottemann and Smogorzewska, 2013). FANCD2 activation is essential for genome integrity maintenance upon double DNA strand break or interstrand crosslinking by favoring the homologous recombination (HR) DNA repair pathway.

BM failure and leukemia at a young age are the hallmarks of human FA patients, which made the study of FA of high interest for understanding the biology of HSC defect and malignant transformation. Mouse models have been developed for several FA genes (Parmar et al., 2009). Despite the mild phenotypes and absence of BM failure in a steady-state condition, FA mouse models present hypersensitivity to DNA-damaging agents, oxidative stress and a deficiency of HSC repopulation abilities (Parmar et al., 2009). Studies of these mouse models have allowed advances in understanding factors and pathways involved in HSC normal functions and BM failure. For example, the study of FANCD2 interaction partners has demonstrated the importance of FOXO3a/FANCD2 interaction in HSC maintenance and resistance against oxidative stress (Li et al., 2010, 2015). Recently, a study emphasizing the relationship between DNA damage and HSC impairment has shown that repeated stresses led to the accumulation of DNA damage and acceleration of functional impairment in FA HSCs (Walter et al., 2015). Despite this accumulation of knowledge about BM failure, potent treatment for FA patients is still needed. Unbiased genomic approaches by short hairpin RNA (shRNA) screens have been successfully used to discover new mechanisms in different pathologies (Mohr et al., 2014), and can be conducted at a stem cell level (Hope et al., 2010; Wang et al., 2012). Using such a strategy, several tumor suppressors and checkpoint factors have been highlighted, such as p53 and p21. Interestingly, several of these proteins have also been implicated in tissue aging and stem cell functions.

In this study, we took advantage of the well-established defective repopulation of FA HSCs and carried out an in vivo shRNA screening in the *Fancd2* mouse model to identify genes whose inhibition would improve HSC functions during replicative stress. We demonstrated that deregulated Pparγ activity is a limiting factor for HSC

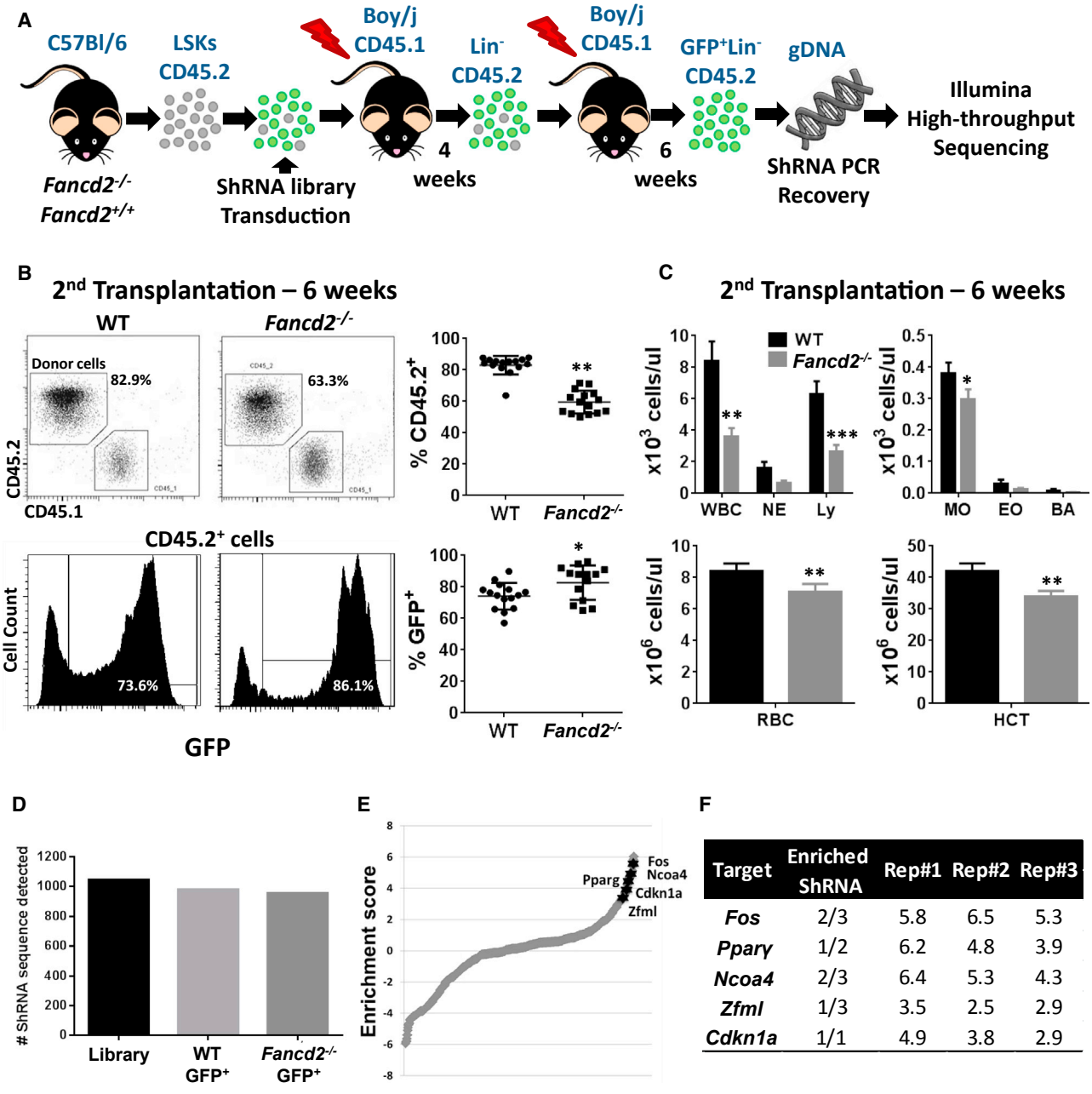


| Target | Enriched ShRNA | Rep#1 | Rep#2 | Rep#3 |
|---|---|---|---|---|
| *Fos* | 2/3 | 5.8 | 6.5 | 5.3 |
| *Pparγ* | 1/2 | 6.2 | 4.8 | 3.9 |
| *Ncoa4* | 2/3 | 6.4 | 5.3 | 4.3 |
| *Zfml* | 1/3 | 3.5 | 2.5 | 2.9 |
| *Cdkn1a* | 1/1 | 4.9 | 3.8 | 2.9 |

**Figure 1. In Vivo shRNA Screening Reveals Candidate Targets in Pparγ Pathway**

(A) Isolated LSKs from 8- to 12-week-old *Fancd2*$^{-/-}$ or *Fancd2*$^{+/+}$ mice (n = 21/genotype) were transduced in vitro with a pooled shRNA lentivirus library. Transduced LSKs along with non-transduced LSKs were transplanted for two rounds into lethally irradiated Boy/J recipient mice (n = 18/groups, three different experiments). Six weeks after the second transplantation, CD45.2$^{+}$Lin$^{-}$GFP$^{+}$ cells were isolated and integrated shRNA sequences were analyzed by deep sequencing.

(B) Plots and graphs represent the percentage of donor cells in blood at 6 weeks after the second transplantation (top) and the percentage of GFP$^{+}$ cells in these donor cells (bottom).

(C) Bar graphs represent the results of blood analysis by Hemavet (Drew Scientific) of recipient mice 6 weeks after the second transplantation (n = 18 mice/genotype). WBC, white blood cells; NE, neutrophils; Ly, lymphocytes; Mo, monocytes; Eo, eosinophils; Ba, basophils; RBC, red blood cells; HCT, hematocrit.

(D) Numbers of shRNA detected by deep sequencing in the cells used to produce the lentivirus particle (library) and Lin$^{-}$ BM cells after the second round of transplantation.

*(legend continued on next page)*

self-renewal and repopulating capacity. Pparγ could be a potent target for improving and delaying FA BM failure and HSC aging in general.

## RESULTS

### In Vivo shRNA Screening Identifies Proteins Involved in TGF-β and PPARγ Pathways

To identify new factors and pathways implicated in impaired functions of HSCs under stress conditions, we conducted an shRNA in vivo screening on transplanted *Fancd2*$^{+/+}$ (wild-type [WT]) and *Fancd2*$^{-/-}$ Lin$^{-}$Sca1$^{+}$Kit$^{+}$ cells (LSKs) (n = 21 donors/group, Figure 1A). To maximize the efficiency of the screening, we used *Fancd2*-deficient mice as they have the strongest phenotypes (Parmar et al., 2009) and HSPC deficiency compared with other FA mice used in our laboratory (Figures S1A and S1B). The shRNA library used in this screen was derived from previously published studies (Bric et al., 2009; Wang et al., 2012). The shRNA lentiviral vector used for the screening expressed a recombinant GFP protein, allowing a fast evaluation of transduction efficiency of the LSKs and the sorting of shRNA-expressing donor cells after transplantation (Figures S2A and S2B). Pooled LSKs (CD45.2) from WT or *Fancd2*$^{-/-}$ mice were transduced in vitro with a similar transduction efficiency of 70%–75% in both genotypes (Figure S2) and then transplanted (Figure 1A) into lethally irradiated recipients (CD45.1). A decreased blood donor chimerism (Figure 1B) and different blood parameters (Figure 1C) were observed for the mice transplanted with *Fancd2*$^{-/-}$ cells at 6 weeks after the second round of transplantation. Thus, the transduction of LSKs with the shRNA library did not rescue by itself the expected phenotype of *Fancd2*-deficient BM cells, suggesting that the experimental model is suitable for selection of beneficial shRNA. We observed a significant increase of GFP$^{+}$ cells among donor cells of *Fancd2*$^{-/-}$ recipient mice at 6 weeks after the second round of transplantation (Figure 1B), indicating a possible selection of cells transduced by beneficial shRNAs.

We isolated CD45.2$^{+}$GFP$^{+}$Lin$^{-}$ cells from the secondary transplanted recipient mice and performed deep sequencing to determine the integrated shRNA sequences (Sims et al., 2011) (Figure S2). We found that the majority of the shRNAs were still present in the sorted cells of both genotypes (Figure 1D) when compared with the virus-producing cells, indicating no random loss of shRNAs during the experiment. The enrichment analysis conducted using ShRNAseq Pipeline (Sims et al., 2011) indicated the selection or loss of shRNAs in recipient mice of Fancd2$^{-/-}$ cells compared with the recipient of WT cells (Table S1 and Figure 1E). Significantly, we found enrichment of three targeted genes of the transforming growth factor β (TGF-β) pathway, *Fos* (Zhang et al., 1998), *Elf* (Chang et al., 2000), and *Klf10* (Spittau and Krieglstein, 2012) (Figures S3B and S3C), and four targeted genes of the PPARγ pathway, *Fos* (Wan et al., 2007), *Ncoa4* (Heinlein et al., 1999), *Pparγ*, and *Zfml* (Meruvu et al., 2011) (Figures 1E and 1F; Table S1).

### Specific shRNA Knockdown of Identified Genes Improves Repopulation Activity of *Fancd2*$^{-/-}$ HSCs

To validate the target genes identified by our screening strategy, we transduced WT and *Fancd2*$^{-/-}$ LSKs with shRNAs targeting the specific genes identified in our in vivo screen. We decided to focus on the *Pparγ*-related genes, because the pathway is the most enriched in our screen and because PPARγ is already a therapeutic target that could be interesting for clinical use (Schmidt et al., 2010). LSK cells were infected with Scramble or shRNA for each target gene (Figures 2A and S3A) to reach 20%–30% transduction efficiency and transplanted into lethally irradiated recipient mice. We followed the percentage of GFP$^{+}$ in donor-derived blood cells as a function of time as an indicator of repopulation efficiency. As shown in Figures 2B and S3D, knocking down *Pparγ*, *Ncoa4* or *Fos* led individually to an increased GFP$^{+}$ proportion in *Fancd2*$^{-/-}$ blood donor-derived cells as a function of time. We confirmed for *Pparγ* that the shRNA vector was able to sustain a stable knockdown for at least 16 weeks (Figure S3E). We also confirmed the deleterious effect of *Klf10* knockdown (Figure 2B and Table S1). As a non-specific control, we used a non-enriched shRNA targeting the nuclear receptor *Nr2c1* and found no significant difference of GFP$^{+}$ proportion 16 weeks after transplantation (Figure 2C).

Furthermore, we performed serial BM transplantation assays and confirmed the increased repopulation activity of *shPparγ*-transduced *Fancd2*$^{-/-}$ HSCs in secondary and tertiary recipient mice (Figure 2D). Interestingly, after the third round of transplantation we also found an increase of GFP$^{+}$ proportion in *shPparγ*-transduced WT blood donor-derived cells compared with scramble *shRNA*-transduced cells (Figure 2D). This result indicates a possible benefit of *Pparγ* knockdown during repeated replicative

(E) Graph showing the enrichment score profile (mean of three independent experiments) of all shRNA detected in Lin$^{-}$ BM cells, highlighting the four genes linked to the Pparγ pathway.

(F) This table depicts for each Pparγ linked candidate genes the number of targeting enriched shRNA (enrichment score >2) and the enrichment score of the best shRNA (according to mean value) into the three replicates.

WT, wild-type. Values are presented as mean ± SD. *p < 0.05, **p < 0.01, ***p < 0.001.

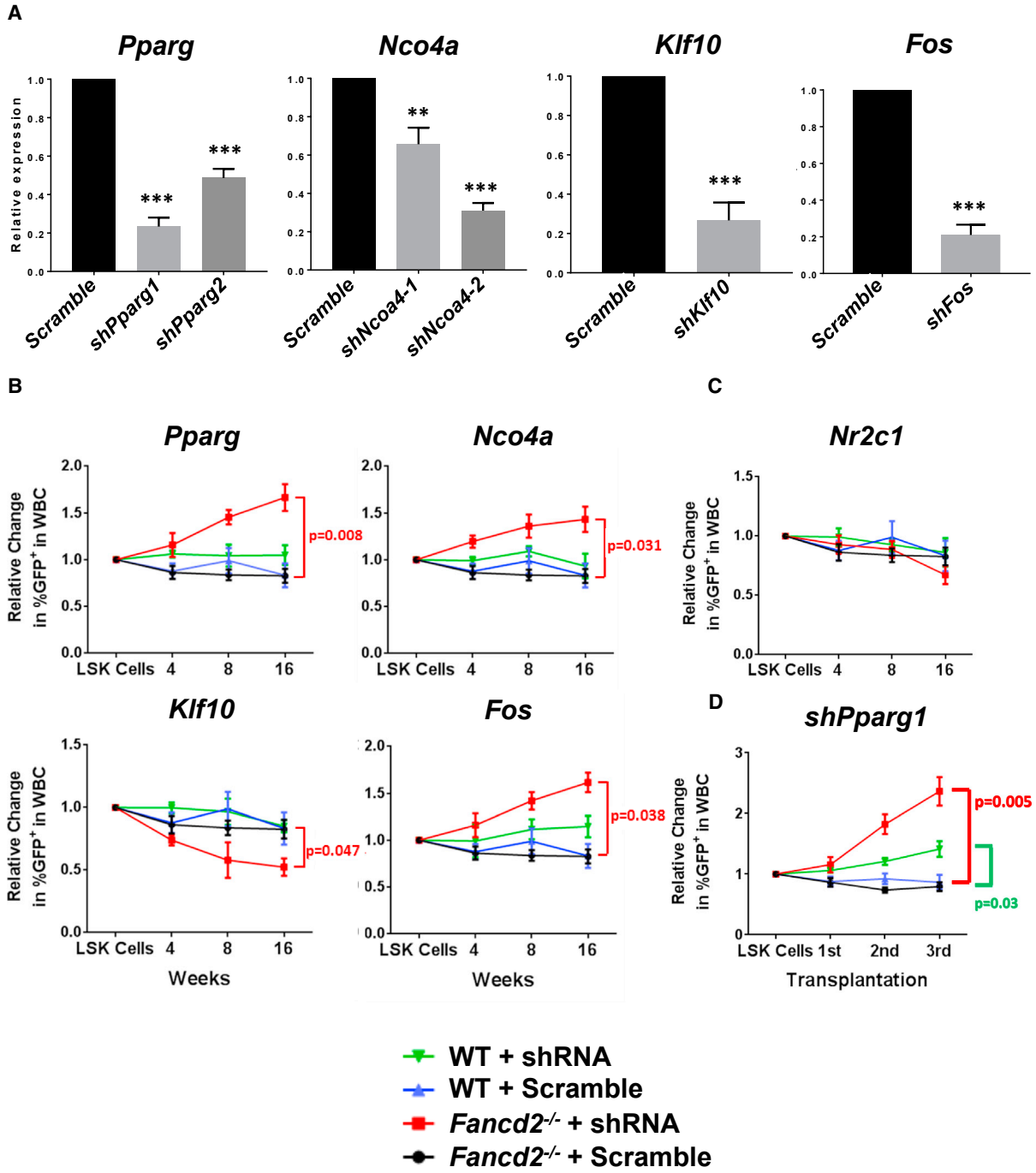


**Figure 2. Specific shRNA Knockdown of PPARγ-Related Candidate Genes Ameliorates Repopulation Capacity of Fancd2$^{-/-}$ LSKs**

(A) Real-time qPCR validation of shRNA efficiency in transduced LSK cells for the different constructs designed to target the indicated genes. Values are presented as mean ± SD. **p < 0.01, ***p < 0.001.

(B–D) Isolated LSKs from *Fancd2*$^{+/+}$ or *Fancd2*$^{-/-}$ mice (n = 6 donors/group, two independent experiments) were transduced with a specific shRNA construct or scrambled shRNA control. The transduction efficiency was 25%–33% before transplantation and was normalized to 1. Transduced cells along with untransduced cells were transplanted into lethally irradiated Boy/J (n = 8 mice/group, two independent experiments). The graphs indicate relative changes in GFP$^{+}$ proportion among donor-derived blood cells (CD45.2) at different time points after transplantation (B and C), or 4 weeks of serial rounds of transplantations (D). Values are presented as mean ± SD.

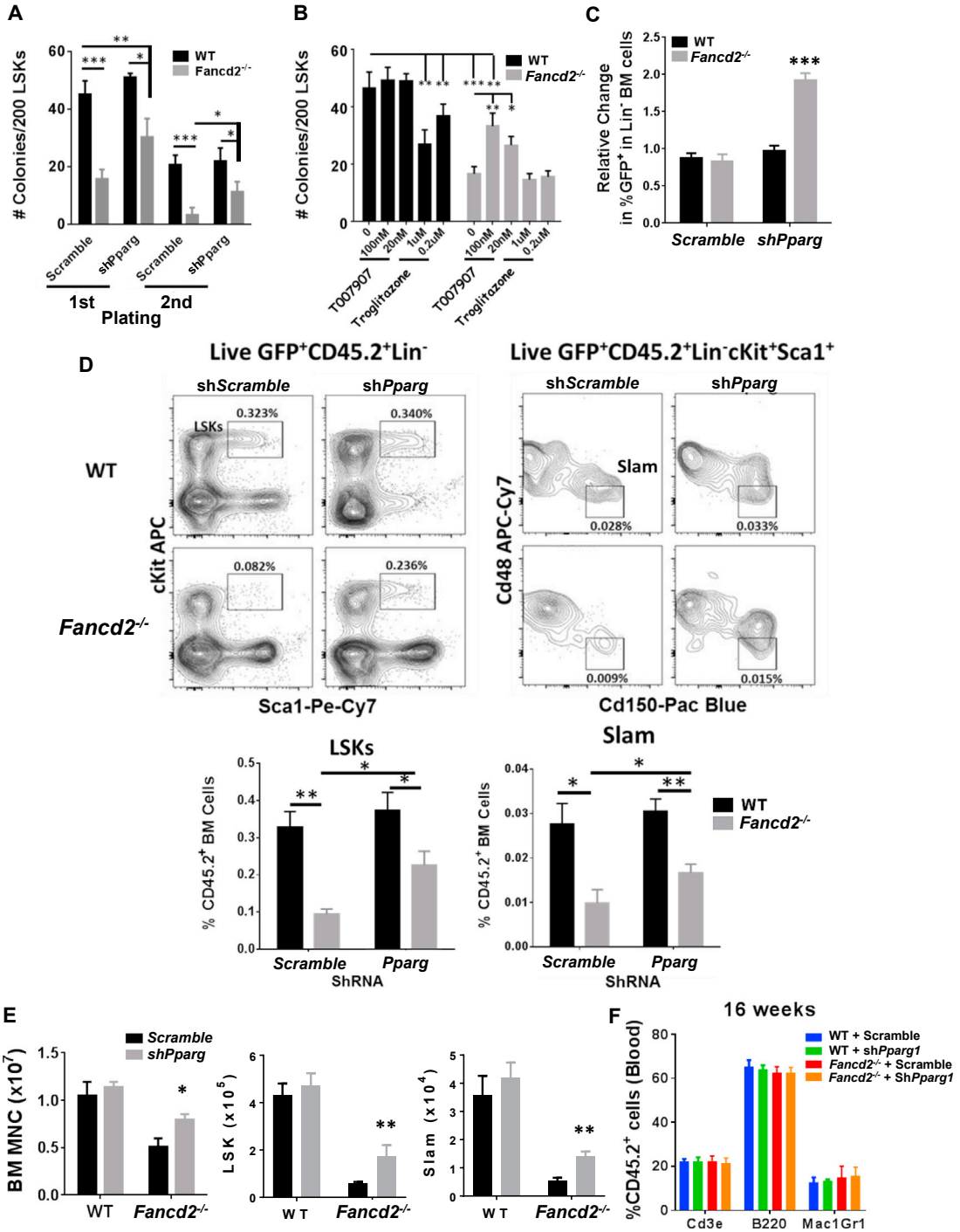


**Figure 3. Inhibition of PPARγ Activity Improves HSC Self-Renewal and BM Repopulation Capacity**

(A and B) CFU assay with LSK cells after shRNA knockdown (A) or treatment with the PPARγ agonist (troglitazone) or antagonist (T0070907) (B).

(C) LSKs isolated from *Fancd2*$^{+/+}$ or *Fancd2*$^{-/-}$ mice (n = 5 donors/group, two independent experiments) were transduced with shRNA targeting *Pparγ* or scrambled shRNA control. The transduction efficiency was 25%–33% before transplantation and was normalized to 1. Transduced cells, along with untransduced cells, were transplanted into lethally irradiated Boy/J (n = 8 mice/group, two independent experiments). The graph shows relative changes in GFP$^{+}$ proportion among donor-derived Lin$^{-}$ BM cells (CD45.2) at 16 weeks after transplantation.

*(legend continued on next page)*

stress on normal HSCs. Together, these results confirmed that specific knockdown of the targeted genes identified in the in vivo shRNA screen has an impact on the repopulation activity of *Fancd2*$^{-/-}$ HSCs, and that PPARγ could be a potential target for improvement of repopulation capacity and function of Fancd2$^{-/-}$ HSCs.

### PPARγ Activation Impaired Function of Both WT and *Fancd2*-Deficient HSPCs

Next, we evaluated the effect of PPARγ inhibition on the function of HSPCs in vitro and in vivo. As expected, we observed with the *shScramble* a decrease in colony numbers for *Fancd2*$^{-/-}$ LSKs compared with WT LSKs after the first or second passage (Figure 3A). Targeting WT LSKs by *shPparγ* did not change the colony number during the first or second passage (Figure 3A). In contrast, *Pparγ* knockdown in *Fancd2*$^{-/-}$ LSKs led to a significant increase in colony number compared with *shScramble* in both the first and second round of culture. The *Fancd2*$^{-/-}$ LSK-derived colonies remained significantly lower than those of WT LSKs (Figure 3A). To confirm this result and to evaluate a possible pharmacological targeting of PPARγ activity in HSPCs, we used the well-characterized PPARγ antagonist T0070907 (Lee et al., 2002) and agonist troglitazone (Lee and Olefsky, 1995). Inhibition of PPARγ activity did not affect the colony number of WT LSK cells at 20 or 100 nM (Figure 3B). However, treatment by T0070907 significantly increased the colony-forming ability of *Fancd2*$^{-/-}$ LSKs, indicating a partial rescue when compared with WT LSKs. Significantly, we found a dose-dependent decrease in colonies formed by WT LSKs treated with the PPARγ agonist, indicating that the activation of PPARγ is sufficient to inhibit the colony-forming capacity of WT LSKs in vitro. Interestingly, troglitazone treatment had no effect on *Fancd2*$^{-/-}$ colony number, indicating that Pparγ activation is probably already at maximum in these cells.

We next evaluated the consequence of Pparγ inhibition on HSC function in vivo. We transduced the WT and *Fancd2*$^{-/-}$ LSKs with *shScramble* or *shPparγ* lentivirus and transplanted the cells into lethally irradiated recipient mice. We evaluated the repopulating capacity of the donor HSCs by analyzing the percentage of GFP$^+$ in recipient mice at 4 months post transplantation. We observed a markedly increased proportion of GFP$^+$Lin$^-$ cells in the BM of the recipient mice transplanted with the *shPparγ*-transduced *Fancd2*$^{-/-}$ LSKs compared with the recipient of *shScramble*-transduced cells (Figure 3C). shRNA knockdown of *Pparγ* in WT LSKs did not change the GFP$^+$ proportion of BM cells in recipient mice compared with *shScramble*-transduced cells. Consistent with previous reports (Ceccaldi et al., 2012; Li et al., 2015; Parmar et al., 2010), recipient mice transplanted with the *shScramble*-transduced *Fancd2*$^{-/-}$ LSKs had a decreased total number of donor-derived mononuclear cells as well as a decreased proportion and absolute number of LSKs and HSCs (SLAM, CD150$^+$CD48$^-$LSK) in the BM at 16 weeks after transplantation compared with mice receiving the *shScramble*-transduced WT LSKs (Figures 3D and 3E). Importantly, shRNA inhibition of Pparγ in *Fancd2*$^{-/-}$ LSKs led to not only a significant increase in total BM cells but also an augmentation of proportion and absolute number of LSKs and HSCs in the transplanted mice compared with *shScramble*-transduced *Fancd2*$^{-/-}$ LSKs (Figures 3D and 3E). The increased repopulation upon *Pparγ* knockdown did not lead to biased lineage commitment, as the different lineage proportions in the CD45$^+$ blood cells is the same in all the conditions tested (Figure 3F). Altogether, these data indicate a deleterious effect of PPARγ activation on HSC function and suggest the potential benefit of PPARγ inhibition on *Fancd2*$^{-/-}$ HSCs.

### Elevated Expression of PPARγ Co-activators and Target Genes in *Fancd2*$^{-/-}$ HSPCs

To determine the mechanism underlying deregulated PPARγ activity in Fancd2-deficient HSPCs, we evaluated the expression of PPARγ co-activators and target genes in donor-derived LSK cells 2 weeks after transplantation. At that time, the HSPCs were under a high proliferative and inflammatory stress because of the need to reconstitute the damaged hematopoietic system (Roy et al., 2012). Surprisingly, we observed no difference in the expression for the two *Pparγ* variant mRNAs in sorted CD45.2$^+$ WT and *Fancd2*$^{-/-}$ LSKs from transplanted mice (Figure 4A). Since it has been described that *Pparγ* expression is not always a good indicator of activity, we evaluated the expression of the PPARγ co-activators *Ncoa4* (Heinlein et al., 1999), *Pparγc1a* (Puigserver et al., 1998), and *Pparγc1b* (Lin et al., 2002). We observed significantly increased expression of *Pparγc1a* and *Ncoa4* in donor-derived Fancd2$^{-/-}$ LSKs at 2 weeks post transplantation (Figure 4A). Interestingly, *Ncoa4* was one of the hits in our shRNA screening (Figure 2B). We also analyzed our microarray data obtained with freshly isolated phenotypic HSCs (CD150$^+$CD48$^-$LSK;

(D–F) Transduced GFP$^+$ LSKs were sorted and transplanted into lethally irradiated Boy/J recipient mice. (D) Representative plot and histograms depict the LSK (Lin$^-$Sca1$^+$cKit$^+$) and SLAM (CD48$^-$CD150$^+$LSKs) percentage among GFP$^+$ mononuclear donor-derived cells (CD45.2) at 16 weeks after transplantation. (E) Absolute number of BM MNC, LSKs, and SLAM cells at 16 weeks after sorted LSK transplantation. (F) Lymphocytes (Cd3e), B cells (B220), and granulocytes (Gr1Mac1) population percentage into CD45$^+$ cells from the blood of 16-week transplanted mice.

WT, wild-type. Values are presented as mean ± SD. *p < 0.05, **p < 0.01, ***p < 0.001.

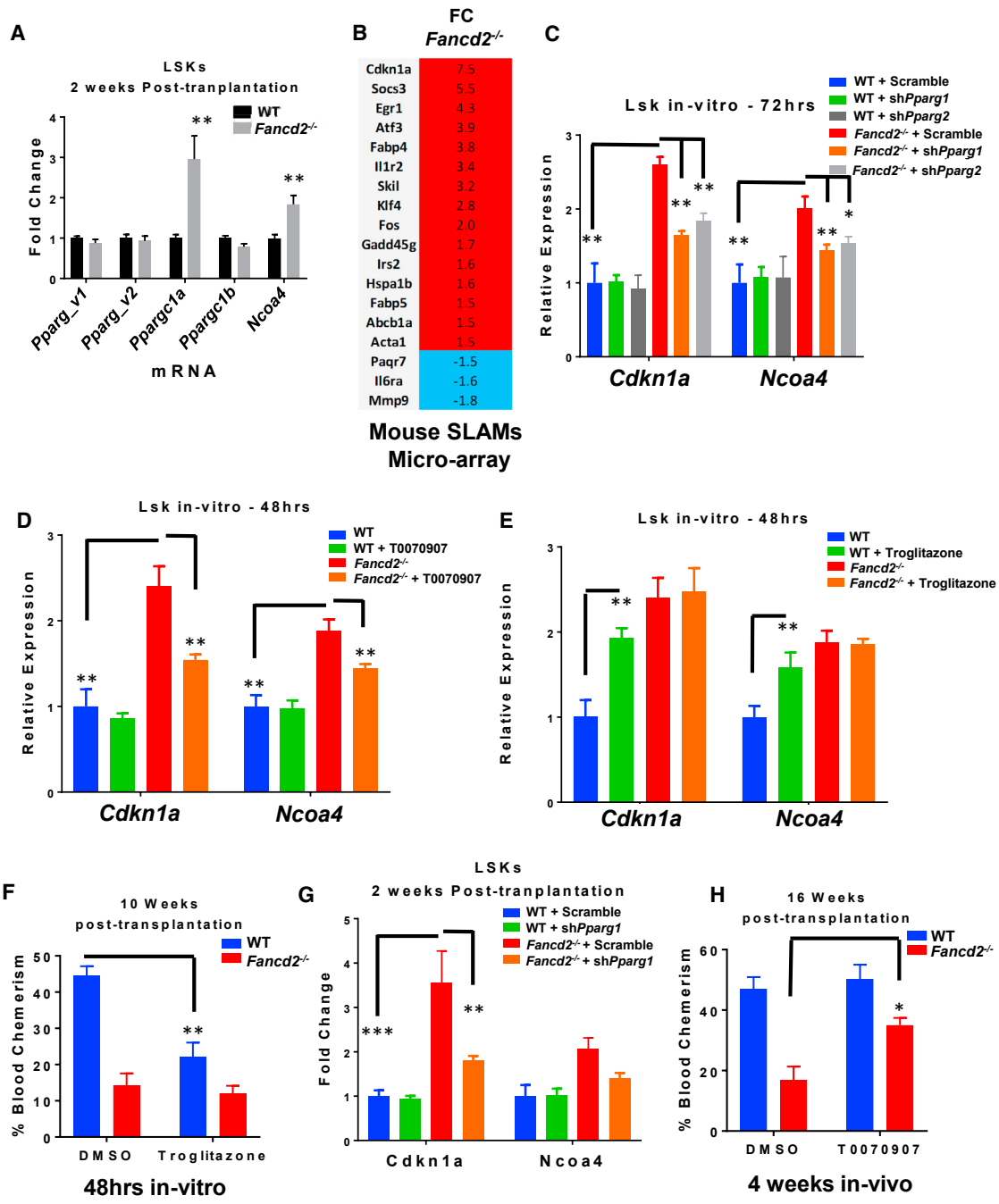


**Figure 4. Deregulated Expression of *Pparγ* and PPARγ Co-activators in *Fancd2*$^{-/-}$ HSPCs**

(A) Real-time qPCR measurement of indicated genes in sorted LSKs 2 weeks after transplantation of LSKs from 8- to 12-week-old *Fancd2*$^{-/-}$ or *Fancd2*$^{+/+}$ mice (n = 4/genotype) into lethally irradiated Boy/J recipient mice (n = 6 mice/group, two independent experiments).

(B) Deregulated Pparγ target genes from previously published *Fancd2*$^{-/-}$ and *Fancd2*$^{+/+}$ SLAM microarray.

(C–E) Real-time qPCR mRNA measurement of indicated genes in *Fancd2*$^{-/-}$ or *Fancd2*$^{+/+}$ LSKs (n = 4/genotype) transduced by *shScramble* or *shPparγ* (C), or in presence or absence of 100 nM T0070907 (D) or 1 μM troglitazone (E).

(F) LSKs from 8- to 12-week-old *Fancd2*$^{-/-}$ or *Fancd2*$^{+/+}$ mice (n = 4 mice/genotype) were treated for 48 hr with 1 μM troglitazone, and 2,000 live cells were transplanted into lethally irradiated Boy/J mice along with CD45.1 competitor BM recipient cells. The bar graph depicts the blood chimerism (CD45.2$^{+}$ cells) of recipient mice 10 weeks after transplantation.

*(legend continued on next page)*

SLAM) from WT and *Fancd2*$^{-/-}$ mice (Li et al., 2015) (GEO: GSE64215). Several *Pparγ* target genes are deregulated in the *Fancd2*$^{-/-}$ SLAM population (Figure 4B). We did not observe in this microarray the deregulation of *Ncoa4* or *Pparγc1a*, suggesting the possible requirement for higher stress conditions to upregulate their expression. As previously reported in FA-deficient cells (Barroca et al., 2012; Ceccaldi et al., 2012), we found upregulation of *Cdkn1a* (p21) in *Fancd2*$^{-/-}$ SLAM cells in the Slam microarray (Figure 4B). Moreover, shRNA targeting *Cdkn1a* was enriched in our shRNA screen (Figure 1 and Table S1).

To validate the regulation of *Cdkn1a* and *Ncoa4* expression by PPARγ, we inhibited or activated PPARγ activity by genetic or pharmacological approaches. Under steady-state conditions, *Fancd2*$^{-/-}$ LSKs showed elevated expression of *Cdkn1a* and *Nco4* compared with WT LSKs (Figures 4C–4E). Inactivation of PPARγ by either shRNA or by treatment with the antagonist T0070907 led to significant reduction of *Cdkn1a* and *Ncoa4* in *Fancd2*-deficient LSKs compared with WT LSKs (Figures 4C and 4D). We treated WT LSK cells with troglitazone and found that activation of Pparγ increased the expression of *Cdkn1a* and *Ncoa4* (Figure 4E). In accordance with the colony assay, we were unable to find a difference in *Cdkn1a* and *Ncoa4* expression after treatment in *Fancd2*$^{-/-}$ LSKs. These data support the notion that PPARγ regulates *Cdkn1a* and *Ncoa4* expression in HSPCs.

The observation that activation of PPARγ by troglitazone increased the expression of *Cdkn1a* in WT LSKs prompted us to ask whether activation of PPARγ inhibited HSPC repopulation capacity. To this end, we treated WT and *Fancd2*$^{-/-}$ LSKs ex vivo with troglitazone and evaluated the hematopoietic repopulating capacity of the treated HSPCs using a BM transplantation assay. At 10 weeks after transplantation, troglitazone-treated WT HSPCs were less efficient in repopulating the irradiated recipients than untreated WT LSKs (Figure 4F). Interestingly, activation of PPARγ in *Fancd2*$^{-/-}$ HSCs did not further impair the repopulation activity. No difference in apoptosis was observed in LSKs treated with troglitazone during 48 hr (data not shown). Thus, the impaired repopulation does not seem to be linked to increased cell death before transplantation. To validate in vivo our in vitro data, we transplanted lethally irradiated mice with WT or *Fancd2*$^{-/-}$ LSKs transduced by *shScramble* or *shPparγ*, along with recipient competitor LSKs. As observed in vitro, inactivation of PPARγ by shRNA led to a decreased expression of *Cdkn1a* and *Ncoa4* at 2 weeks post transplantation (Figure 4G). We further confirmed the beneficial role of PPARγ inhibition on *Fancd2*$^{-/-}$ HSPCs by treating transplanted mice with the antagonist T0070907 during the first 4 weeks after irradiation, when the donor cells are subjected to a high level of replicative stress due to rigorous BM repopulation. As observed with *Pparγ* shRNA knockdown, in vivo inhibition of PPARγ activity by T0070907 led to a partial rescue of Fancd2$^{-/-}$ HSC repopulation capacity (Figure 4H). Long-term evaluation of transplanted mice showed an extended life span of mice receiving *shPparγ*-transduced Fancd2$^{-/-}$ LSKs compared with mice receiving *shScramble*-transduced *Fancd2*$^{-/-}$ LSKs (Figure S3F). Notably, after 1 year no sign of leukemia was observed as depicted by the white blood cell count at 50 weeks (Figure S3G). Altogether, these data indicate that HSPCs are able to respond to aberrant PPARγ activity and that PPARγ activation under replicative stress impairs FA HSPC function, likely through upregulating *Cdkn1a* expression.

## Upregulated *PPARγ* and Its Co-activators in FA Patient-Derived Cell Lines and Primary FA Patient Samples

We next evaluated whether our findings in the mouse model were extendable to humans. We first compared the expression of *PPARγ*, *NCOA4*, *CDKN1a*, and *PPRγC1a* in human *FANCD2*-deficient lymphoblastic cell lines genetically complemented (PD20$^{WT}$) or not (PD20$^{Vect}$) by WT human *FANCD2* cDNA. We observed a significant increase in the expression of *NCOA4*, *CDKN1a*, and *PPARγC1a* in *FANCD2*-deficient cells compared with the complemented cells (Figure 5A). Since antioxidant treatment is able to ameliorate PD20 FA phenotypes (Li et al., 2012, 2014; Ponte et al., 2012), we decided to evaluate the expression of the *PPARγ*-related genes in response to treatment with hydrogen peroxide ($H_2O_2$). Oxidative stress increased expression of *CDKN1a* and *PPARγC1a* (Figure 5B). Interestingly, treatment with $H_2O_2$ elevated the expression of *NCOA4*, indicating a link between oxidative stress and this *PPARγ* co-activator. However, $H_2O_2$ treatment did not increase the expression of *PPARγ* in PD20$^{WT}$ cells (Figure 5B). It is possible that oxidative stress affects the activity of PPARγ, not its gene expression. To test this notion, we inhibited PPARγ activity using T0070907 in PD20$^{WT}$ cells

(G) Real-time qPCR measurement in sorted LSKs 2 weeks after transplantation of LSKs from 8- to 12-week-old *Fancd2*$^{-/-}$ or *Fancd2*$^{+/+}$ mice transduced with *shScramble* or *shPparγ* into lethally irradiated Boy/J recipient mice (n = 4 mice/group).
(H) LSKs were sorted from 8 to 12 weeks old *Fancd2*$^{-/-}$ or *Fancd2*$^{+/+}$ mice (n = 4 mice/genotype), and 2,000 sorted LSKs (CD45.2) were transplanted into lethally irradiated Boy/J mice along with 2,000 competitor LSKs (CD45.1). Mice were injected intraperitoneally every other day with T0070907 (5 mg/kg) or control vehicle (DMSO) (n = 4 mice/group) during the first 4 weeks after transplantation. The bar graph depicts the blood chimerism (CD45.2$^+$ cells) of recipient mice 16 weeks after transplantation.
WT, wild-type. Values are presented as mean ± SD. *p < 0.05, **p < 0.01, ***p < 0.001.

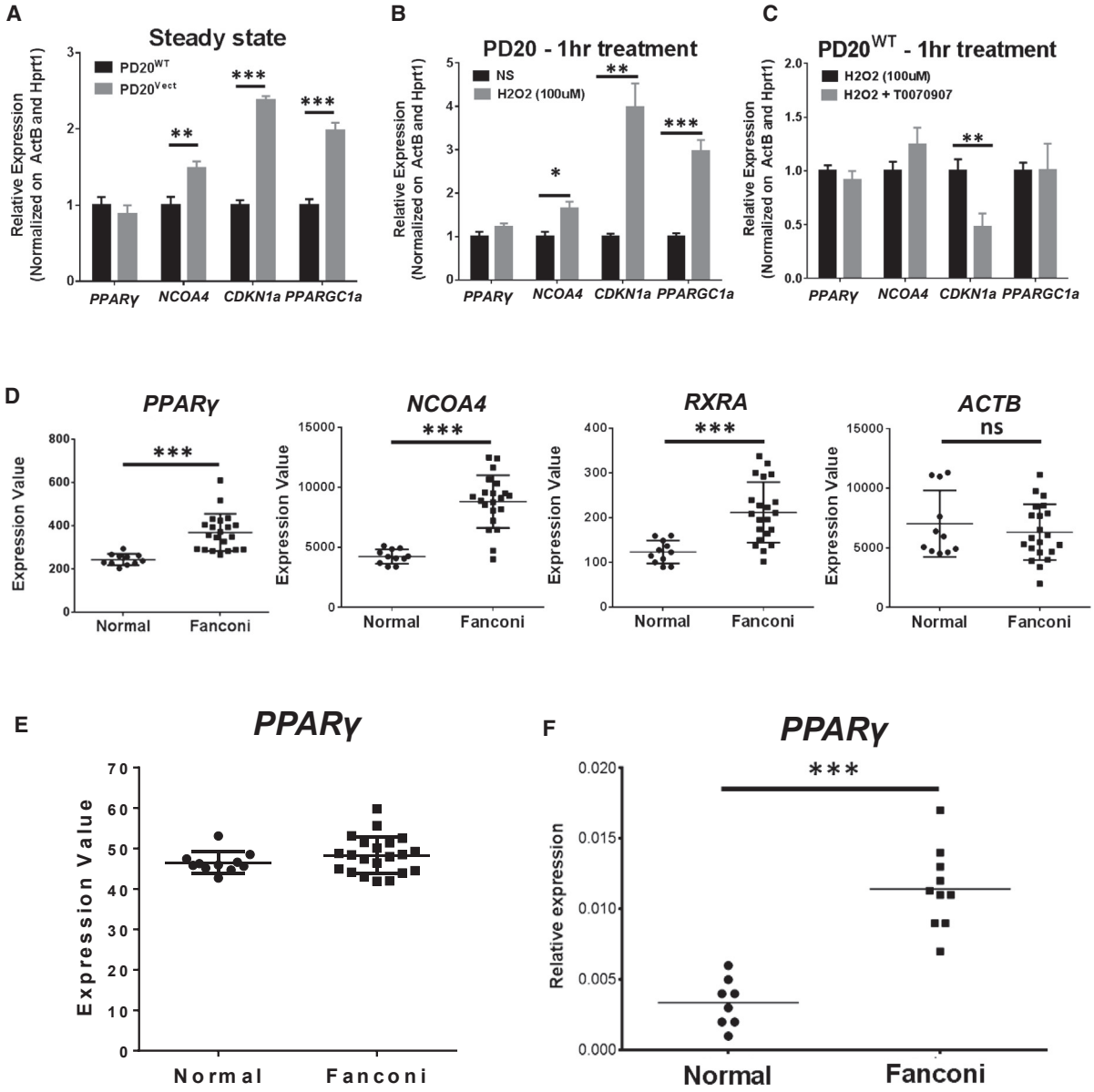


**Figure 5. Deregulated PPARγ in Human FA-Deficient Cells**

(A) Real-time qPCR mRNA measurement of indicated genes in *FANCD2*-deficient ($PD20^{vect}$) or *FANCD2*-complemented ($PD20^{WT}$) human lymphoblastic cell lines (three independent experiments).

(B) Real-time qPCR mRNA measurement of indicated genes in $PD20^{WT}$ treated with or without 100 μM $H_2O_2$ (three independent experiments).

(C) Real-time qPCR mRNA measurement of indicated genes in $PD20^{WT}$ treated with or without 100 μM $H_2O_2$ in the presence or absence of 100 nM T0070907 (three independent experiments).

(D and E) Analysis of *PPARγ*-related genes and *ACTB* control in previously published microarray on BM cells from normal donors or FA patients.

(F) Real-time qPCR measurement of *PPARγ* mRNA in BM $CD34^+$ cells from normal (n = 8) or FA patients (n = 10).

Values are presented as mean ± SD. *p < 0.05, **p < 0.01, ***p < 0.001. ns, not significant.

exposed to $H_2O_2$. Inhibition of PPARγ significantly reduced the expression of *CDKN1a* upon $H_2O_2$ treatment (Figure 5C), indicating that PPARγ participates in the regulation of this gene in response to oxidative stress. PPARγ inhibition did not change the expression of *NCOA4* and *PPARγC1a* (Figure 5C).

To substantiate the human relevance further, we analyzed the published transcriptome data derived from

BM cells of a large cohort of FA patients (GEO: GSE16334) (Vanderwerf et al., 2009) for PPARγ-related genes. Interestingly, we found significantly increased expression of *CDKN1a* and *NCOA4* in FA patients (Figure 5D). While we did not find upregulation of *PPARγ* (Figure 5E) and *PPARγC1a* (data not shown), we found upregulation of *RXRa* (Figure 5D), a gene encoding another co-activator of PPARγ (Mangelsdorf and Evans, 1995). Furthermore, we observed by real-time qPCR a significant elevation in the expression of *PPARγ* in BM HSPCs ($CD34^+$) isolated from a small cohort of FA patients compared with the samples from healthy donors (Figure 5F). Together, these data suggest that consistent with its role in *Fancd2*$^{-/-}$ HSPCs, deregulated PPARγ activity may contribute to BM pathology in FA patients.

## DISCUSSION

The current study provides several pieces of evidence that abnormal Pparγ activation in HSCs leads to HSC function impairment under replicative stress. (1) shRNA against *Pparγ* and *Pparγ*-related genes were enriched in *Fancd2*-deficient HSPCs undergoing hematopoietic repopulation. (2) Specific knockdown of *Pparγ* improved the repopulation capacity of *Fancd2*-deficient HSCs. (3) Genetic or pharmacological inhibition of Pparγ decreased expression of *Cdkna1a* in mouse and human FA-deficient cells and improved the repopulation capacity of *Fancd2*-deficient HSCs.

PPARγ is a central transcription factor regulating adipocyte differentiation and energy metabolism (Siersbaek et al., 2010). Interestingly, increased population of adipocytes in the BM has been observed in FA patients and mouse models (Pulliam-Leath et al., 2010), suggesting a possible dysregulation of PPARγ. Moreover, it has been shown that adipocytes are deleterious for HSC self-renewal (Naveiras et al., 2009). These observations are in accordance with our current study demonstrating that pharmacological or intrinsic activation of PPARγ impaired hematopoietic repopulation of *Fancd2*-deficient HSCs as well as WT HSCs. In this context, it is noteworthy that our recent study (Amarachintha et al., 2015) with *Fanca*- and *Fancd2*-deficient BM mesenchymal stromal cells revealed upregulation of PPARγ activity and *Pparγc1a* expression and adipocyte differentiation in FA, suggesting that hyperactivation of PPARγ could be a common feature of FA cells. In accordance with a deleterious effect of PPARγ on the hematopoietic system, development of anemia in humans has been shown to be a side effect after the introduction of a PPARγ agonist drug on the market (Werner and Travaglini, 2001). In addition, FA patients are frequently treated with androgens, which delay BM failure (Dokal, 2003). Interestingly, androgen and PPARγ signaling inhibit each other (Dokal, 2003; Du et al., 2009; Singh et al., 2006). Thus, the effectiveness of androgen treatment in FA patients may be in part related to PPARγ inhibition, although this hypothesis has to be investigated.

Since the p53/p21 axis has been described as an impairment mechanism of FA-deficient HSCs and also plays important roles in other models of HSC aging (Choudhury et al., 2007), we evaluated the effect of PPARγ on *CDKN1a* expression. We found that inhibition of PPARγ downregulated the expression of *CDKNA1a* in *FANCD2*-deficient human lymphoblast cell line (PD20) and mouse *Fancd2*$^{-/-}$ HSPC (LSK) cells. PPARγ interacts and activates p53 to upregulate p21 expression (Han et al., 2003) and can bind directly to the *TP53* promoter to increase p53 expression (Bonofiglio et al., 2006). Interestingly, the levels of the p53 protein are known to be upregulated in *FANCD2*-deficient PD20 cells and *Fancd2*$^{-/-}$ mouse LSK cells (Ceccaldi et al., 2012). In connection with PPARγ and p53 interaction, PPARγ activation leads to an increase in cell-cycle arrest and apoptosis in different cancer cell types (Burstein et al., 2003; Mueller et al., 2000; Theocharisa et al., 2003). In this context, we speculate a possible linkage between PPARγ activation and upregulation of p21 through p53 upregulation. Since direct targeting of p53 or p21 is not a safe therapeutic strategy, treatments that modulate the p53/p21 activity might improve HSC functions while maintaining vital tumor-suppressive functions. In supporting this notion, we kept lethally irradiated recipient mice reconstituted with Scramble or *shPparγ* -transduced *Fancd2*$^{-/-}$ LSK cells for 1 year without detecting leukemia development.

Surprisingly, we did not observe an alteration in *PPARγ* expression in *FANCD2*-deficient PD20 cells and HSPCs or the published FA patient BM microarray. However, we detected overexpression of *PPARγ* in human FA $CD34^+$ BM cells, suggesting that modulation of *PPARγ* expression might be more important in primitive HSCs. Since PPARγ level in either gene expression or total protein is not always a good indicator of its activity, we evaluated the expression of PPARγ co-activators. We found significantly increased expression of NCOA4, a known co-activator of PPARγ (Heinlein et al., 1999) and a hit in our screen, in mouse *Fancd2*-deficient LSKs after transplantation and in BM cells of an FA patient. This similarity in the mouse model and human samples suggests a possible deleterious role of PPARγ in humans. Nevertheless, no functional assessment has been conducted on human HSPCs in this study, and further studies are needed to confirm the relevance of PPARγ signaling in primary human cells and patients.

Little is known about the relationship between NCOA4 and PPARγ beyond transcriptional co-activation. In this study, we showed that PPARγ regulated the expression of *NCOA4* under oxidative or replicative stress. Interestingly,

it has been recently reported that inhibition of NCOA4 confers resistance to oxidative stress (Mancias et al., 2014). We and others have described the hypersensitivity of FA-deficient cells to oxidative stress (Pagano et al., 2012). Moreover, we have shown that treatment of FA mice with the antioxidant quercetin can ameliorate the FA phenotype (Li et al., 2014), and a pilot study on the use of quercetin in FA patients is in progress at the Cincinnati Children's Hospital. Thus, it is possible that the upregulation of *NCOA4* in FA-deficient cells has a direct impact on PPARγ activation and sensitivity to oxidative stress. Another link between PPARγ and oxidative stress comes from the direct activation of PPARγ by oxidative stress (Polvani et al., 2012). In fact, oxidative stress is a known inducer of PPARγ activity. PPARγ is believed to play a protective role against oxidative stress under physiological conditions. The increased levels of reactive oxygen species (ROS) in FA cells could be responsible for an increased and sustained activation of PPARγ that could impair HSC functions. In support of this notion, we found that treatment of human cells with $H_2O_2$ elevated the expression of the PPARγ-related genes such as *NCOA4*, *CDKN1a*, and *PPARγC1a*, and that activation of PPARγ in WT murine LSKs impaired their repopulation activities. Finally, we observed an upregulation of *PPARγC1a* in *Fancd2*-deficient mouse LSKs as well as in *FANCD2*-deficient PD20 cells. PPARγC1a can act as co-stimulator of PPARγ (Puigserver et al., 1998), which has an important role in mitochondrial biogenesis (Wu et al., 1999). Emerging evidence shows that FA deficiency leads to damaged mitochondria (Pagano et al., 2012, 2014). It is conceivable that when repopulating the BM upon stress, HSCs would have to enter the cell cycle that requires enhanced mitochondrial activity to meet high energy demand, which would increase ROS production. We speculate that because of damaged and less efficient mitochondria, the FA-deficient HSCs need to increase mitochondrial biogenesis to meet energy demand. Therefore, upregulation of *PPARγC1a* in FA may be due to mitochondrial damages leading to increased accumulation of ROS, which in turn activates PPARγ.

In summary, using an in vivo shRNA screen in donor HSCs, we identified a deleterious effect of deregulated Pparγ activity on HSC functions. Modulation by pharmaceutical compounds of PPARγ signaling is potentially a therapeutic modality in a large proportion of patients with blood diseases, including FA.

## EXPERIMENTAL PROCEDURES

### Mice

Mice were maintained in a pathogen-free environment in the Cincinnati Children's Hospital Medical Center (CCHMC) mouse housing facility. The protocols of animal experiments were approved by the Institutional Animal Care and Use Committee at CCHMC. *Fancd2*$^{+/-}$ mice were provided by Dr. Markus Grompe (Oregon Health & Sciences University) (Houghtaling et al., 2003). When indicated, mice were injected intraperitoneally with the PPARγ inhibitor T0070907 (5 mg/kg) or with control vehicle (DMSO) as indicated in the figure legends.

### Bone Marrow Transplantation

Congenic CD45.1 mice were lethally irradiated (12 Gy) and intravenously injected on the same day with whole mononuclear BM cells or isolated Lin$^-$ or Lin$^-$Sca1$^+$cKit$^+$ (LSK) BM cells from donor mice. For competitive transplantation, 500 LSKs (CD45.2) were transplanted with 0.3 million congenic BM cells.

### Flow Cytometry and Cell Sorting

BM cells isolated from the femurs and tibias of mice were labeled on ice (for antibody details see Supplemental Experimental Procedures). Propidium iodide (PI) was used to detect dead cells. Live Lin$^-$ or LSK cells (PI$^-$Lin$^-$Sca1$^+$cKit$^+$) were sorted from mice BM using a FACSAria II (BD Bioscience). Lin$^-$, LSK, and Slam cells (CD48$^-$CD150$^+$ LSK cells) were detected by flow cytometry on a BD Fortessa cytometer (BD Biosciences). CD45.1 and CD45.2 labeling were used to distinguish recipient and donor-derived BM or blood cells.

### Cell Culture

Sorted LSKs were cultured in Stem Span SFEM medium (STEMCELL Technologies) supplemented with 100 ng/mL murine stem cell factor and 50 ng/mL murine thrombopoietin (Preprotech). The Pparγ agonist troglitazone or antagonist T0070907 (Cayman) were added at the initiation of culture at the concentration indicated on the figures. For colony-forming assay, 200 LSKs or $5 \times 10^3$ MNC BM cells were cultured into cytokines supplemented Methocult3434 medium (STEMCELL). Colonies were counted on day 7 and replated for the second round in the same condition.

### shRNA Library and Vector Construction

The shRNA library pool was provided by Dr. Lenhard Rudolph (Max-Planck-Research Institute) (Wang et al., 2012). Construction details about SFFVΔEcoR1-Egfp-shRNA vector use in specific gene silencing are provided in Supplemental Experimental Procedures.

### LSK Transduction and In Vivo Screening

A schematic experimental flow of the LSK transduction for shRNA screening is depicted in Figure S1. In brief, sorted *Fancd2*$^{-/-}$ or *Fancd2*$^{+/+}$ LSKs were cultured in 96-well round-bottomed low-attachment plates (BD Biosciences). A total of 20,000 LSKs/well were transduced 12 hr after culture ignition to obtain 70%–75% (MOI = 20) or 20%–30% (MOI = 5) transduction efficiency. For in vivo screening, 20,000–25,000 pooled transduced LSK cells were transplanted into lethally irradiated recipient mice. Four weeks after transplantation, CD45.2$^+$Lin$^-$ BM cells were sorted and transplanted for a second round into recipient mice. Six weeks later, CD45.2$^+$GFP$^+$Lin$^-$ BM cells were sorted for genomic DNA extraction using the Gentra PureGene Blood Kit (QIAGEN).

### Integrated shRNA Detection and Enrichment Analysis

We adapted the protocol and primers previously described (Sims et al., 2011) (Figure S2 and Supplemental Experimental Procedures). FASTQ files generated after sequencing of screening were mapped to the shRNA library sequence using the ShAlign Perl program (Sims et al., 2011). The enrichment score of each shRNA sequence was calculated using the ShRNAseq R package (Sims et al., 2011).

### Real-Time qPCR

Total RNA was isolated from cells in culture or freshly sorted LSKs with the RNeasy plus mini kit (QIAGEN). Reverse transcription of total mRNA was obtained using The High Capacity cDNA kit (Applied Biosystems). qPCR was conducted on an ABI 7900 (Applied Biosystems). Primers for qPCR are listed in Figure S4.

### Statistical Analysis

Student's t test was used for two-group comparison and one-way ANOVA for more than two-group comparison using the Tukey post hoc test to correct for multiple comparisons with GraphPad Prism software. Values of $p < 0.05$ were considered statistically significant. Results are presented as mean ± SD. Values in the figures are depicted as $^{*}p < 0.05$, $^{**}p < 0.01$, and $^{***}p < 0.001$.

## SUPPLEMENTAL INFORMATION

Supplemental Information includes Supplemental Experimental Procedures and one table, and four figures and can be found with this article online at http://dx.doi.org/10.1016/j.stemcr.2017.03.008.

## AUTHOR CONTRIBUTIONS

M.S.: Conception and design, collection and assembly of data, data analysis and interpretation, manuscript writing. W.D.: Collection and assembly of data, data analysis and interpretation. S.A.: Collection and assembly of data. A.W.: Collection of data. Q.P.: Conception and design, manuscript writing, final approval of manuscript.

## ACKNOWLEDGMENTS

We thank Drs. Lenhard Rudolph and Jianwei Wang (Germany Research Group on Stem Cell Aging, Germany) for the shRNA library and helpful suggestions about this work, and Dr. Markus Grompe (Oregon Health & Sciences University) for Fancd2$^{+/-}$ mice, the Comprehensive Mouse and Cancer Core of the Cincinnati Children's Research Foundation (CCHMC) for bone marrow transplantation service, and the Viral Vector Core of Cincinnati Children's Research Foundation (CCHMC) for the preparation of lentiviruses. We also thank members of the Q.P. laboratory for helpful discussions and Ms. Samantha Losekamp for editing the manuscript. This work was supported by NIH grants R01 HL076712 and R01 CA157537. Q.P. is supported by a Leukemia and Lymphoma Scholar award.

Received: August 5, 2016
Revised: March 9, 2017
Accepted: March 10, 2017
Published: April 13, 2017

## REFERENCES

Amarachintha, S., Sertorio, M., Wilson, A., Li, X., and Pang, Q. (2015). Fanconi anemia mesenchymal stromal cells-derived glycerophospholipids skew hematopoietic stem cell differentiation through toll-like receptor signaling. Stem Cells *33*, 3382–3396.

Barroca, V., Mouthon, M.A., Lewandowski, D., Brunet de la Grange, P., Gauthier, L.R., Pflumio, F., Boussin, F.D., Arwert, F., Riou, L., Allemand, I., et al. (2012). Impaired functionality and homing of Fancg-deficient hematopoietic stem cells. Hum. Mol. Genet. *21*, 121–135.

Bonofiglio, D., Aquila, S., Catalano, S., Gabriele, S., Belmonte, M., Middea, E., Qi, H., Morelli, C., Gentile, M., Maggiolini, M., et al. (2006). Peroxisome proliferator-activated receptor-gamma activates p53 gene promoter binding to the nuclear factor-kappaB sequence in human MCF7 breast cancer cells. Mol. Endocrinol. *20*, 3083–3092.

Bric, A., Miething, C., Bialucha, C.U., Scuoppo, C., Zender, L., Krasnitz, A., Xuan, Z., Zuber, J., Wigler, M., Hicks, J., et al. (2009). Functional identification of tumor-suppressor genes through an in vivo RNA interference screen in a mouse lymphoma model. Cancer Cell *16*, 324–335.

Burstein, H.J., Demetri, G.D., Mueller, E., Sarraf, P., Spiegelman, B.M., and Winer, E.P. (2003). Use of the peroxisome proliferator-activated receptor (PPAR) gamma ligand troglitazone as treatment for refractory breast cancer: a phase II study. Breast Cancer Res. Treat *79*, 391–397.

Ceccaldi, R., Parmar, K., Mouly, E., Delord, M., Kim, J.M., Regairaz, M., Pla, M., Vasquez, N., Zhang, Q.S., Pondarre, C., et al. (2012). Bone marrow failure in Fanconi anemia is triggered by an exacerbated p53/p21 DNA damage response that impairs hematopoietic stem and progenitor cells. Cell Stem Cell *11*, 36–49.

Chang, J., Lee, C., Hahm, K.B., Yi, Y., Choi, S.G., and Kim, S.J. (2000). Over-expression of ERT(ESX/ESE-1/ELF3), an ets-related transcription factor, induces endogenous TGF-beta type II receptor expression and restores the TGF-beta signaling pathway in Hs578t human breast cancer cells. Oncogene *19*, 151–154.

Choudhury, A.R., Ju, Z., Djojosubroto, M.W., Schienke, A., Lechel, A., Schaetzlein, S., Jiang, H., Stepczynska, A., Wang, C., Buer, J., et al. (2007). Cdkn1a deletion improves stem cell function and lifespan of mice with dysfunctional telomeres without accelerating cancer formation. Nat. Genet. *39*, 99–105.

Dokal, I. (2003). Inherited aplastic anaemia. Hematol. J. *4*, 3–9.

Du, J., Zhang, L., and Wang, Z. (2009). Testosterone inhibits the activity of peroxisome proliferator-activated receptor gamma in a transcriptional transaction assay. Pharmazie *64*, 692–693.

Han, C., Demetris, A.J., Michalopoulos, G.K., Zhan, Q., Shelhamer, J.H., and Wu, T. (2003). PPARgamma ligands inhibit cholangiocarcinoma cell growth through p53-dependent GADD45 and p21 pathway. Hepatology *38*, 167–177.

Heinlein, C.A., Ting, H.J., Yeh, S., and Chang, C. (1999). Identification of ARA70 as a ligand-enhanced coactivator for the peroxisome proliferator-activated receptor gamma. J. Biol. Chem. *274*, 16147–16152.

Hope, K.J., Cellot, S., Ting, S.B., MacRae, T., Mayotte, N., Iscove, N.N., and Sauvageau, G. (2010). An RNAi screen identifies Msi2

and Prox1 as having opposite roles in the regulation of hematopoietic stem cell activity. Cell Stem Cell *7*, 101–113.

Houghtaling, S., Timmers, C., Noll, M., Finegold, M.J., Jones, S.N., Meyn, M.S., and Grompe, M. (2003). Epithelial cancer in Fanconi anemia complementation group D2 (Fancd2) knockout mice. Genes Dev. *17*, 2021–2035.

Kottemann, M.C., and Smogorzewska, A. (2013). Fanconi anaemia and the repair of Watson and Crick DNA crosslinks. Nature *493*, 356–363.

Lee, M.K., and Olefsky, J.M. (1995). Acute effects of troglitazone on in vivo insulin action in normal rats. Metabolism *44*, 1166–1169.

Lee, G., Elwood, F., McNally, J., Weiszmann, J., Lindstrom, M., Amaral, K., Nakamura, M., Miao, S., Cao, P., Learned, R.M., et al. (2002). T0070907, a selective ligand for peroxisome proliferator-activated receptor gamma, functions as an antagonist of biochemical and cellular activities. J. Biol. Chem. *277*, 19649–19657.

Li, J., Du, W., Maynard, S., Andreassen, P.R., and Pang, Q. (2010). Oxidative stress-specific interaction between FANCD2 and FOXO3a. Blood *115*, 1545–1548.

Li, J., Sipple, J., Maynard, S., Mehta, P.A., Rose, S.R., Davies, S.M., and Pang, Q. (2012). Fanconi anemia links reactive oxygen species to insulin resistance and obesity. Antioxid. Redox Signal *17*, 1083–1098.

Li, X., Li, L., Li, J., Sipple, J., Schick, J., Mehta, P.A., Davies, S.M., Dasgupta, B., Waclaw, R.R., and Pang, Q. (2014). Concomitant inactivation of foxo3a and fancc or fancd2 reveals a two-tier protection from oxidative stress-induced hydrocephalus. Antioxid. Redox Signal *21*, 1675–1692.

Li, X., Li, J., Wilson, A., Sipple, J., Schick, J., and Pang, Q. (2015). Fancd2 is required for nuclear retention of Foxo3a in hematopoietic stem cell maintenance. J. Biol. Chem. *290*, 2715–2727.

Lin, J., Puigserver, P., Donovan, J., Tarr, P., and Spiegelman, B.M. (2002). Peroxisome proliferator-activated receptor gamma coactivator 1beta (PGC-1beta ), a novel PGC-1-related transcription coactivator associated with host cell factor. J. Biol. Chem. *277*, 1645–1648.

Mancias, J.D., Wang, X., Gygi, S.P., Harper, J.W., and Kimmelman, A.C. (2014). Quantitative proteomics identifies NCOA4 as the cargo receptor mediating ferritinophagy. Nature *509*, 105–109.

Mangelsdorf, D.J., and Evans, R.M. (1995). The RXR heterodimers and orphan receptors. Cell *83*, 841–850.

Meruvu, S., Hugendubler, L., and Mueller, E. (2011). Regulation of adipocyte differentiation by the zinc finger protein ZNF638. J. Biol. Chem. *286*, 26516–26523.

Mohr, S.E., Smith, J.A., Shamu, C.E., Neumüller, R.A., and Perrimon, N. (2014). RNAi screening comes of age: improved techniques and complementary approaches. Nat. Rev. Mol. Cell Biol. *15*, 591–600.

Morrison, S.J., Uchida, N., and Weissman, I.L. (1995). The biology of hematopoietic stem cells. Annu. Rev. Cell Dev. Biol. *11*, 35–71.

Mueller, E., Smith, M., Sarraf, P., Kroll, T., Aiyer, A., Kaufman, D.S., Oh, W., Demetri, G., Figg, W.D., Zhou, X.P., et al. (2000). Effects of ligand activation of peroxisome proliferator-activated receptor gamma in human prostate cancer. Proc. Natl. Acad. Sci. USA *97*, 10990–10995.

Naveiras, O., Nardi, V., Wenzel, P.L., Hauschka, P.V., Fahey, F., and Daley, G.Q. (2009). Bone-marrow adipocytes as negative regulators of the haematopoietic microenvironment. Nature *460*, 259–263.

Orford, K.W., and Scadden, D.T. (2008). Deconstructing stem cell self-renewal: genetic insights into cell-cycle regulation. Nat. Rev. Genet. *9*, 115–128.

Orkin, S.H., and Zon, L.I. (2008). Hematopoiesis: an evolving paradigm for stem cell biology. Cell *132*, 631–644.

Pagano, G., Talamanca, A.A., Castello, G., Pallardó, F.V., Zatterale, A., and Degan, P. (2012). Oxidative stress in Fanconi anaemia: from cells and molecules towards prospects in clinical management. Biol. Chem. *393*, 11–21.

Pagano, G., Shyamsunder, P., Verma, R.S., and Lyakhovich, A. (2014). Damaged mitochondria in Fanconi anemia—an isolated event or a general phenomenon? Oncoscience *1*, 287–295.

Parmar, K., D'Andrea, A., and Niedernhofer, L.J. (2009). Mouse models of Fanconi anemia. Mutat. Res. *668*, 133–140.

Parmar, K., Kim, J., Sykes, S.M., Shimamura, A., Stuckert, P., Zhu, K., Hamilton, A., Deloach, M.K., Kutok, J.L., Akashi, K., et al. (2010). Hematopoietic stem cell defects in mice with deficiency of Fancd2 or Usp1. Stem Cells *28*, 1186–1195.

Polvani, S., Tarocchi, M., and Galli, A. (2012). PPARγ and oxidative stress: Con(β) catenating NRF2 and FOXO. PPAR Res. *2012*, 641087.

Ponte, F., Sousa, R., Fernandes, A.P., Gonçalves, C., Barbot, J., Carvalho, F., and Porto, B. (2012). Improvement of genetic stability in lymphocytes from Fanconi anemia patients through the combined effect of α-lipoic acid and N-acetylcysteine. Orphanet J. Rare Dis. *7*, 28.

Puigserver, P., Wu, Z., Park, C.W., Graves, R., Wright, M., and Spiegelman, B.M. (1998). A cold-inducible coactivator of nuclear receptors linked to adaptive thermogenesis. Cell *92*, 829–839.

Pulliam-Leath, A.C., Ciccone, S.L., Nalepa, G., Li, X., Si, Y., Miravalle, L., Smith, D., Yuan, J., Li, J., Anur, P., et al. (2010). Genetic disruption of both Fancc and Fancg in mice recapitulates the hematopoietic manifestations of Fanconi anemia. Blood *116*, 2915–2920.

Rossi, D.J., Jamieson, C.H., and Weissman, I.L. (2008). Stem cells and the pathways to aging and cancer. Cell *132*, 681–696.

Roy, S., Javed, S., Jain, S.K., Majumdar, S.S., and Mukhopadhyay, A. (2012). Donor hematopoietic stem cells confer long-term marrow reconstitution by self-renewal divisions exceeding to that of host cells. PLoS One *7*, e50693.

Sawyer, S.L., Tian, L., Kähkönen, M., Schwartzentruber, J., Kircher, M., Majewski, J., Dyment, D.A., Innes, A.M., Boycott, K.M., Moreau, L.A., et al. (2015). Biallelic mutations in BRCA1 cause a new Fanconi anemia subtype. Cancer Discov. *5*, 135–142.

Schmidt, M.V., Brüne, B., and von Knethen, A. (2010). The nuclear hormone receptor PPARγ as a therapeutic target in major diseases. ScientificWorldJournal *10*, 2181–2197.

Siersbaek, R., Nielsen, R., and Mandrup, S. (2010). PPARgamma in adipocyte differentiation and metabolism—novel insights from genome-wide studies. FEBS Lett. *584*, 3242–3249.

Sims, D., Mendes-Pereira, A.M., Frankum, J., Burgess, D., Cerone, M.A., Lombardelli, C., Mitsopoulos, C., Hakas, J., Murugaesu, N., Isacke, C.M., et al. (2011). High-throughput RNA interference screening using pooled shRNA libraries and next generation sequencing. Genome Biol. *12*, R104.

Singh, R., Artaza, J.N., Taylor, W.E., Braga, M., Yuan, X., Gonzalez-Cadavid, N.F., and Bhasin, S. (2006). Testosterone inhibits adipogenic differentiation in 3T3-L1 cells: nuclear translocation of androgen receptor complex with beta-catenin and T-cell factor 4 may bypass canonical Wnt signaling to down-regulate adipogenic transcription factors. Endocrinology *147*, 141–154.

Spittau, B., and Krieglstein, K. (2012). Klf10 and Klf11 as mediators of TGF-beta superfamily signaling. Cell Tissue Res. *347*, 65–72.

Taniguchi, T., and D'Andrea, A.D. (2006). Molecular pathogenesis of Fanconi anemia: recent progress. Blood *107*, 4223–4233.

Theocharisa, S., Margeli, A., and Kouraklis, G. (2003). Peroxisome proliferator activated receptor-gamma ligands as potent antineoplastic agents. Curr. Med. Chem. Anticancer Agents *3*, 239–251.

Vanderwerf, S.M., Svahn, J., Olson, S., Rathbun, R.K., Harrington, C., Yates, J., Keeble, W., Anderson, D.C., Anur, P., Pereira, N.F., et al. (2009). TLR8-dependent TNF-(alpha) overexpression in Fanconi anemia group C cells. Blood *114*, 5290–5298.

Walter, D., Lier, A., Geiselhart, A., Thalheimer, F.B., Huntscha, S., Sobotta, M.C., Moehrle, B., Brocks, D., Bayindir, I., Kaschutnig, P., et al. (2015). Exit from dormancy provokes DNA-damage-induced attrition in haematopoietic stem cells. Nature *520*, 549–552.

Wan, Y., Chong, L.W., and Evans, R.M. (2007). PPAR-gamma regulates osteoclastogenesis in mice. Nat. Med. *13*, 1496–1503.

Wang, J., Sun, Q., Morita, Y., Jiang, H., Gross, A., Lechel, A., Hildner, K., Guachalla, L.M., Gompf, A., Hartmann, D., et al. (2012). A differentiation checkpoint limits hematopoietic stem cell self-renewal in response to DNA damage. Cell *148*, 1001–1014.

Werner, A.L., and Travaglini, M.T. (2001). A review of rosiglitazone in type 2 diabetes mellitus. Pharmacotherapy *21*, 1082–1099.

Wu, Z., Puigserver, P., Andersson, U., Zhang, C., Adelmant, G., Mootha, V., Troy, A., Cinti, S., Lowell, B., Scarpulla, R.C., et al. (1999). Mechanisms controlling mitochondrial biogenesis and respiration through the thermogenic coactivator PGC-1. Cell *98*, 115–124.

Zhang, Y., Feng, X.H., and Derynck, R. (1998). Smad3 and Smad4 cooperate with c-Jun/c-Fos to mediate TGF-beta-induced transcription. Nature *394*, 909–913.

**Stem Cell Reports, Volume *8***

## Supplemental Information

# In Vivo RNAi Screen Unveils PPARγ as a Regulator of Hematopoietic Stem Cell Homeostasis

**Mathieu Sertorio, Wei Du, Surya Amarachintha, Andrew Wilson, and Qishen Pang**

## Suplemental Material and methods

### Antibodies used for Flow cytometry labelling

Antibodies used for labelling were: anti-mouse- CD45.1-Pe-Cy7 or -Fitc (Clone A20, Ebioscience), CD45.2-PE or -Fitc (Clone 104, Ebioscience), Blood Lineage cocktail biotinylated Abs kit (BD Biosciences), Sca1-PeCy7 (Clone D7, Ebioscience), cKit-APC (Clone 2B8, BD Biosciences), CD48-PE (Clone HM48-1, Ebioscience), CD150-Pacific Blue (Clone TC15-12F12.2, Bio Legend), CD3ε-Fitc (Clone 145-2C11, BD biosciences), CD11b-PE (Clone M1/70, BD biosciences), CD45R/B220-Alexa700 (Clone RA3-6B2, BD biosciences), and Ly6G/Ly-6C-APC (Clone RB6-8C5, BD biosciences). Streptavidin-Percp-Cy5.5 (BD Biosciences) was used for detection of biotinylated Abs labelled cells.

### SFFVΔEcoR1-Egfp-ShRNA construction

In order to use the same vector for single ShRNA cloning, the SFFV-eGFP-ShRNA vector used in the library was digested by AsisI and PshAI (New England Biolabs) to remove a second EcoRI restriction site and allowed cloning after EcoRI/XhoI digestion. Digested vector was purified after agarose gel migration and self-ligated using T4 ligase (New England Biolabs) to create the SFFVΔEcoR1-Egfp-ShRNA. Single genes specific sequences were designed with the RNAi codex website (http://cancan.cshl.edu/cgi-bin/Codex/Codex.cgi) using the ShRNA sequence with the best enrichment score from screening. Single genes ShRNA targeting sequences used in this study are depicted in Table S1.

### Lentivirus production

All lentiviruses were produced by the CCHMC viral vector with ShRNA lentiviral vector, pCMVΔR8.91 and pMD.G. Viruses were concentrated by ultracentrifugation and re-suspended in PBS. Virus titer was determined cytometry detection of $GFP^+$ cells 48h after transduction of 293T cells.

**ShRNA sequences recovery and sequencing**

ShRNA integrated sequences were recovered by PCR with a forward primer (link to the P7 Illumina sequence and index sequence = P7+Loop) matching the constant loop in 5' of the antisense ShRNA sequence and a reverse primer (link to the P5 Illumina sequence = P5+Mir30) matching the constant part of the vectors in 3'... PCR was performed using AmpliTaq gold polymerase (Life Technology) in a final reaction volume of 100uL. After 5 minutes denaturation of gDNA at 95°C, PCR was conducted with 25 cycles as follow: Denaturation = 95°C, 30s – Annealing = 54°C, 45s – Extension = 75°C, 30s. PCR products were purified and concentrated after agarose gel migration using a Wizard® SV Gel and PCR Clean-Up System (Promega). Quantification, library preparation and sequencing reaction were conducted by the CCHMC DNA Sequencing core using an Illumina Hi-Seq sequencer with the following sequencing primer: TAGCCCCTTGAATTCCGAGGCAGTAGGCA.

## Supplemental Data

**FigureS1: Repopulation and colony forming unit deficiencies of different FA deficient mice.** (A) Donors BM cells from *Fanca*$^{-/-}$, *Fancc*$^{-/-}$, *Fancd2*$^{-/-}$ or WT mice were transplanted with recipient BM cells (Ratio 1:1) into lethally irradiated Boy/J mice (n=6 mice/genotypes). (B) BM cells from *Fanca*$^{-/-}$, *Fancc*$^{-/-}$, *Fancd2*$^{-/-}$ or WT mice were plated for 2 rounds of CFU assay. The histograms depict the colony number counted at 7 days of each plating (3 mice/genotype).

**FigureS2: In-vivo ShRNA screening strategy and analyze details.** Representation of the strategy used to conduct the in-vivo ShRNA screening on WT and *Fancd2* deficient LSK cells (genotyping on top of figures). LSK cells were sorted and transduced with the 1000 Cancer pool of shRNAs. After 48h, GFP expression was monitored in transduced LSKs, which were transplanted into lethally irradiated Boy/J mice. (B) Step by step pipeline of ShRNA screening analysis used in this paper (derived from Sim et al., 2011). (C) Schematic representation of the PCR and primers used for ShRNA sequence recovery before deep sequencing.

**FigureS3: Figure 2, 3 and 4 supportive data.** (A) Graphic showing the enrichment score profile (mean of 3 independent experiments) of all shRNA detected in Lin$^-$ BM cells, highlighting the 3 genes linked to TGF-Beta. (B) The table depicts for each TGF-Beta linked candidate genes the number of targeting enriched shRNA (enrichment score >2) and the enrichment score of the best shRNA (according to mean value) into the 3 replicates. (C) Validation of Sh*Pparg2* as described in Fig.2. (E) RT-qPCR validation of Sh*Pparg1* efficiency on sorted GFP$^+$Lin$^-$ cells at 4 and 16weeks after transplantation (n=4mice/group). (F) Wt or Fancd2$^{-/-}$ LSKs were sorted and transduced in vitro with ShScramble or sh*Pparg1*. GFP$^+$ cells were sorted 2 days post transduction and transplanted into lethally irradiated mice. Mice were followed for survival during 360 days. Data expressed as percentage of surviving mice. (G) Hemavet white blood cell count at 360 days post transplantation from the mice described in (F).

**FigureS4: List of ShRNA sequences and Primer sequences used in qPCR experiments.** (A) Table showing ShRNA sequences of the different genes targeted in this study and Scrambled ShRNA. (B) Table showing specific forward and reverse primer sequences used for each gene expression evaluated in this study.

**Table S1: Enrichment score of detected ShRNA targeted genes.** Values represent the highest mean enrichment score obtained for each targeted genes.

## Supplemental Figure 1

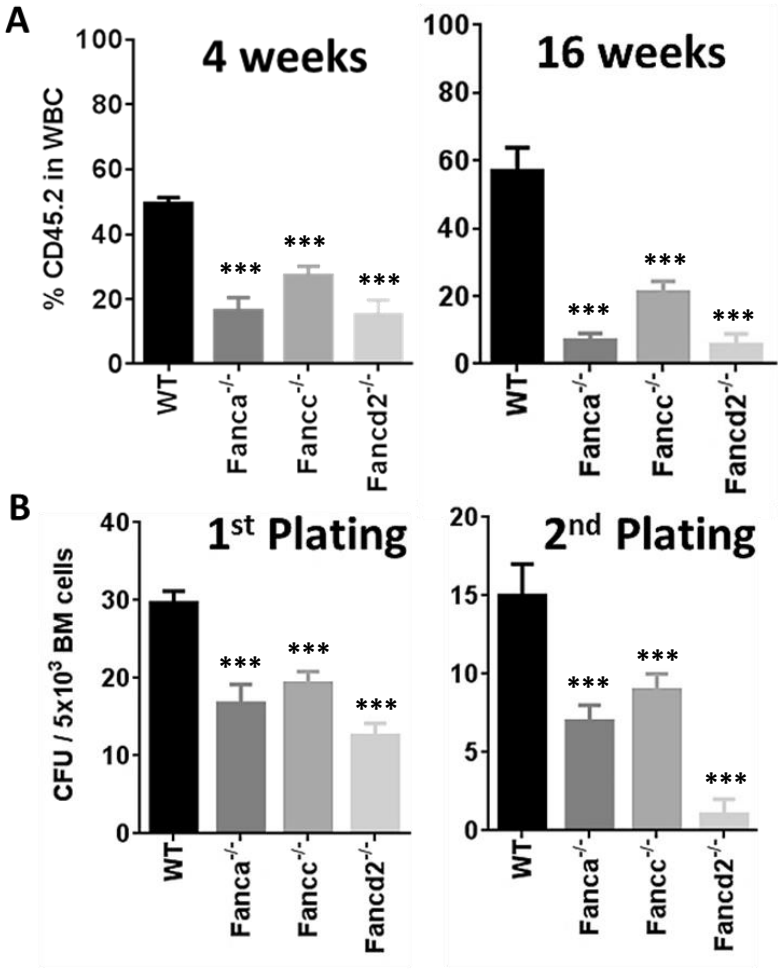

# Supplemental Figure 2

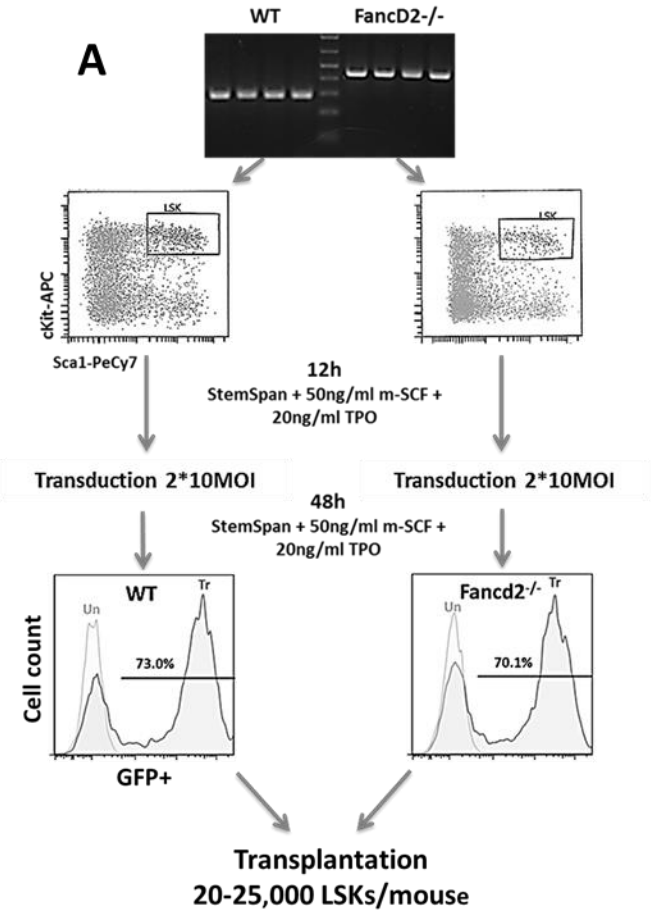


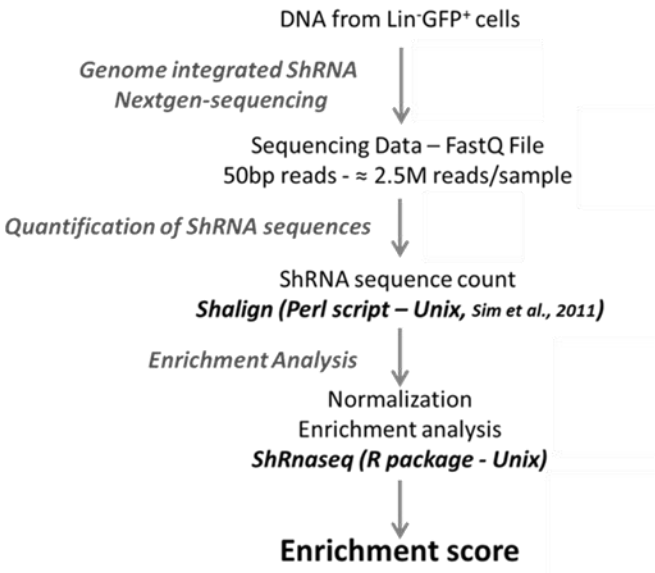


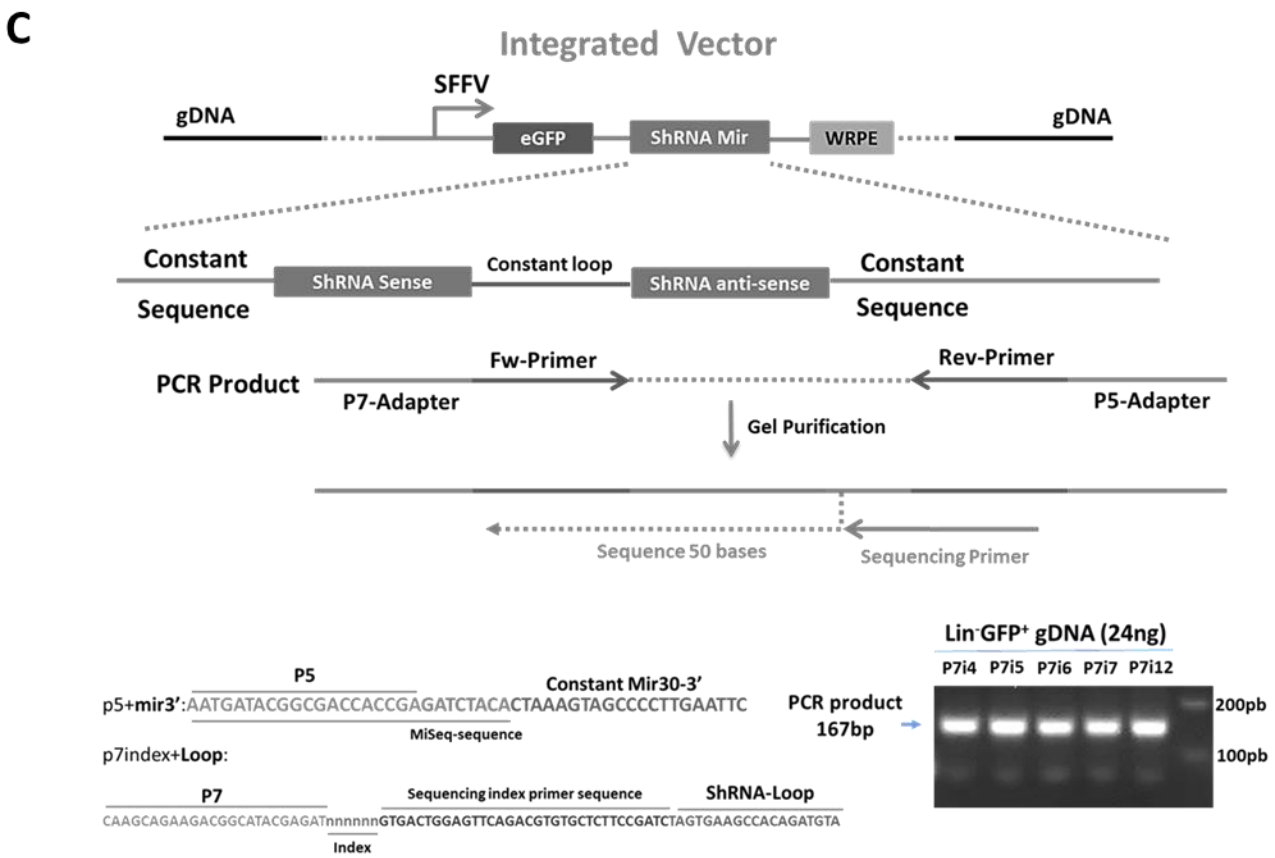

# Supplemental Figure 3

A

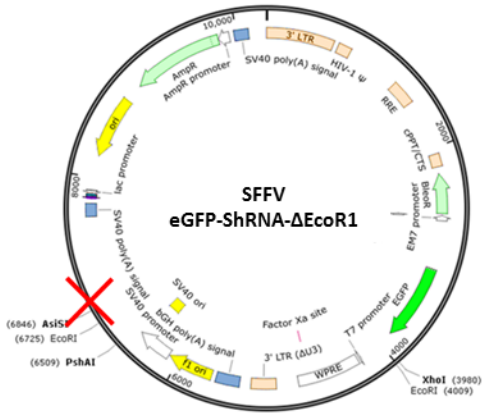


B

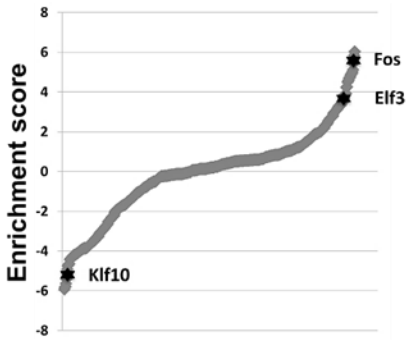


C

| Target | Enriched ShRNA | Rep#1 | Rep#2 | Rep#3 |
|---|---|---|---|---|
| Fos | 2/3 | 5.8 | 6.5 | 5.3 |
| Elf3 | 1/3 | 4.2 | 5.1 | 2.3 |
| Klf10 | 2/3 | -7.4 | -4.3 | -5.1 |

D

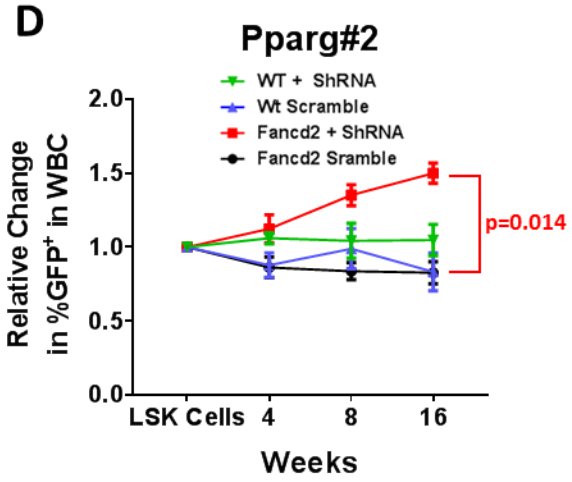


E

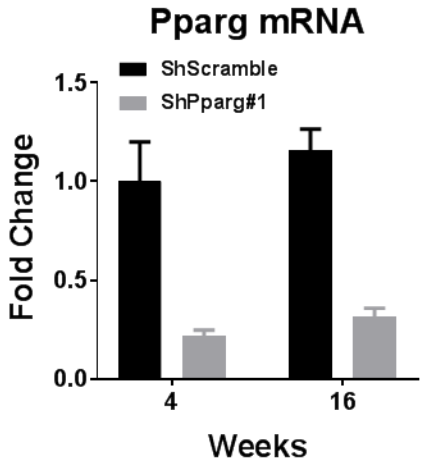


F

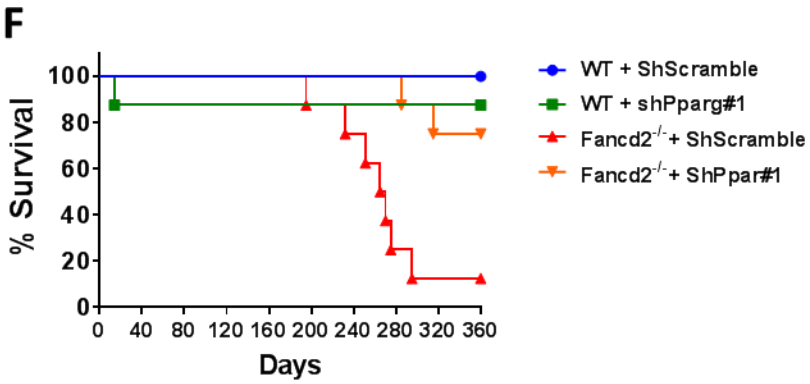


G

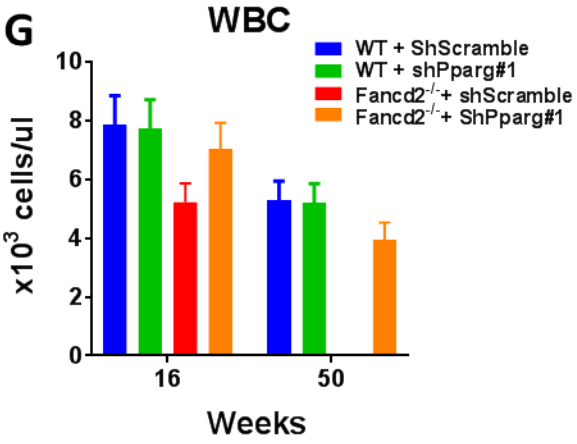

## Supplemental Figure4

**A**

| ShRNA | ShRNA sense sequence |
|---|---|
| sh*Pparg1* | CAATGGTTGCTGATTACAA |
| sh*Pparg2* | GATTGAAGCTTATTTATGA |
| sh*Ncoa4-1* | GAATGCCTATGGAACCTAA |
| sh*Ncoa4-2* | GGCAATCTGAAATGCCTAA |
| sh*Klf10* | GACTGGAAGTCTCATTTCA |
| sh*Fos* | GCAATAGCGTGTTCCAATT |
| Sh*Nr2c1* | GCGTCATTACGGAGCAATA |
| Sh*Scramble* | CTCGCTTGGGCGAGAGTAA |

**B**

| | Primer 5' -> 3' | |
|---|---|---|
| **Gene** | **FW** | **Rev** |
| *mPParg_v1* | TTTTCCGAAGAACCATCCGATT | ATGGCATTGTGAGACATCCCC |
| *mPparg_v2* | TCGCTGATGCACTGCCTATG | GAGAGGTCCACAGAGCTGATT |
| *mNcoa4* | GAACCATCAGGACACATGGAAA | AGGAGCCATAGCCTTGGGT |
| *mPpargc1a* | TATGGAGTGACATAGAGTGTGCT | CCACTTCAATCCACCCAGAAAG |
| *mPpargc1b* | TCCTGTAAAAGCCCGGAGTAT | GCTCTGGTAGGGGCAGTGA |
| *mCdkn1a* | CCTGGTGATGTCCGACCTG | CCATGAGCGCATCGCAATC |
| *mKlf10* | ATGCTCAACTTCGGCGCTT | CGCTTCCACCGCTTCAAAG |
| *mFos* | CGGGTTTCAACGCCGACTA | TTGGCACTAGAGACGGACAGA |
| *mNr2c1* | ATGGCGACCATAGAAGAAATTGC | CAAGTGCTGTCACGATCTGGA |
| *mHprt1* | CGTCGTGATTAGCGATGATG | ACAGAGGGCCACAATGTGAT- |
| *mActb* | GGCTGTATTCCCCTCCATCG | CCAGTTGGTAACAATGCCATGT |
| *hPPARG* | AGAAGCCTGCATTTCTGCAT | TCAAAGGAGTGGGAGTGGTC |
| *hNCOA4* | ACAGTTGCATAAGCCGTCACC | TGAGCCTGCTGTTGAAGTGTC |
| *hPPARGC1a* | TCTGAGTCTGTATGGAGTGACAT | CCAAGTCGTTCACATCTAGTTCA |
| *hPPARGC1b* | GATGCCAGCGACTTTGACTC | ACCCACGTCATCTTCAGGGA |
| *hCDKN1A* | TGTCCGTCAGAACCCATGC | AAAGTCGAAGTTCCATCGCTC |
| *hHPRT1* | GAAAAGGACCCCACGAAGTGT | AGTCAAGGGCATATCCTACAA |
| *hACTB* | CATGTACGTTGCTATCCAGGC | CTCCTTAATGTCACGCACGAT |